IEEE Access
Multidisciplinary | Rapid Review | Open Access Journal

Received 20 October 2022, accepted 6 November 2022, date of publication 14 November 2022, date of current version 23 November 2022.

Digital Object Identifier 10.1109/ACCESS.2022.3222372

RESEARCH ARTICLE

Nonlinearly Activated IEZNN Model for Solving Time-Varying Sylvester Equation

YIHUI LEI[1], JIAMEI LUO[1], TENGXIAO CHEN[1], LEI DING[2], BOLIN LIAO[2], GUANGPING XIA[1], AND ZHENGQI DAI[1]

[1]College of Mathematics and Statistics, Jishou University, Jishou 416000, China
[2]College of Computer Science and Engineering, Jishou University, Jishou 416000, China

Corresponding author: Lei Ding (dinglei@jsu.edu.cn)

This work was supported in part by the National Natural Science Foundation of China under Grant 61966014 and Grant 62066015, and in part by the Research Foundation of Education Bureau of Hunan Province under Grant 20A407.

ABSTRACT Zeroing neural network (ZNN) is an effective method to calculate time-varying problems. However, the ZNN and its extensions separately addressed the robustness and the convergence. To simultaneously promote the robustness and finite-time convergence, a nonlinearly activated integration-enhanced ZNN (NIEZNN) model based on a coalescent activation function (C-AF) has been designed for solving the time-varying Sylvester equation in various noise situations. The C-AF with an optimized structure is convenient for simulations and calculations, which promotes NIEZNN accelerates convergence speed without remarkable efficiency loss. The robustness and the finite-time convergence of the NIEZNN model have been proved in theoretical analyses. Furthermore, the upper bounds of convergence time of the NIEZNN model and the noise-attached NIEZNN model have been deduced in theory. At last, numerical comparative results and the application to mobile manipulator have validated the efficiency and superiority of the NIEZNN model based on the designed coalescent activation function.

INDEX TERMS Zeroing neural network, time-varying Sylvester equation, nonlinear activation functions, robustness, Finite-time convergence.

I. INTRODUCTION

Sylvester equation has a wide field of application in disturbance decoupling [1], image processing [2], linear least square regression [3], control system [4] and robots [5]. Therefore, the study on the solution of Sylvester equation has been investigated greatly [6], [7], [8], [9], [10], [11]. The Bartels-Stewart algorithm is a classical direct method to solve Sylvester equation [12]. Based on this algorithm, some extensions were proposed in [13] and [14]. Nevertheless, the Bartels-Stewart algorithm was proven that it can complete the calculation within a time complexity $O(n^3)$. When used to large-scale real-time application, the Bartels-Stewart algorithm cannot satisfy the requirement. In addition, based on gradient means, a mass of iterative algorithms were exploited to solve Sylvester equation [15], [16], [17], [18]. Those algorithms worked well in static Sylvester equation. However, when applied to the dynamic (i.e. time varying) Sylvester equation, these algorithms fail because the sampling rate is too high in time-varying Sylvester equation.

In recent decades, the recurrent neural network (RNN) as a typical representative of parallel algorithm, was greatly applied in optimization [19], robotics [20], [21], game theory [22], prediction [23]. Different from iterative algorithms, RNN has excellent performance in parallel-distributed processing and convenient hardware implementation. As a competitive computational tool, RNN plays a pivotal role in solving Sylvester equation [4], [24]. According to above literatures, it is known that the solution error of RNN vanished to zero in time-invariant case, and the error failed in vanishing to zero in time-varying case. For overcoming the defect, a special kind of RNN was first proposed in [24], which named zeroing neural network (ZNN). By exploiting the velocity compensation of time-varying coefficients, ZNN can exponentially converge to the theoretical solution of time-varying Sylvester equation [25], [26]. The design formula of

The associate editor coordinating the review of this manuscript and approving it for publication was Yilun Shang.

conventional ZNN (CZNN) is presented as follows:

$$\dot{\mathfrak{E}}(t) = \frac{\mathrm{d}\mathfrak{E}(t)}{\mathrm{d}t} = -\mu\mathfrak{E}(t), \tag{1}$$

where $\mathfrak{E}(t)$ is the error monitoring function, the parameter $\mu > 0$. Due to the significant improvement in convergence property, ZNN was studied deeply. The in-depth study can be mainly summarized into two branches.

One is robustness. Noise is unavoidable in the solution task of ZNN, such as some realization errors in hardware implementation, the environmental disturbance. Sometimes, the noise has significant impacts on the accuracy of ZNN. Therefore, it is worth investigating the robustness of ZNN with different noise. The evolution formula of CZNN has an essential design defect: sensitive to noise [27], [28]. To overcome this flaw, in [27] and [28], the evolution formula was ameliorated by the integral unit as

$$\dot{\mathfrak{E}}(t) = -\mu\mathfrak{E}(t) - \nu\int_0^t \mathfrak{E}(s)\,\mathrm{d}s, \tag{2}$$

where the parameters $\mu > 0$, $\nu > 0$. Due to the design of the integral unit, (2) is named as integration-enhanced ZNN (IEZNN). IEZNN owns a noise-suppression property. The improvement of robustness expanded the practical application of ZNN.

The other is finite-time convergence. As time is valuable in solving time-varying issues, the research on finite-time convergence has became a hot point in the field of ZNN. As noted in literature [29] that appropriate nonlinear activation function can accelerate the convergence. Which inspires researchers to explore certain nonlinear activation functions to improve convergence of ZNN. For example, in [30], [31], [32], [33], and [34], three nonlinear activation functions (i.e. the bi-polar-sigmoid activation function, power activation function and power-sigmoid activation function) were explored and widely adopted. It is worth pointing out that these mentioned nonlinear activation functions have superior convergence speed than the linear one, but cannot actualize the finite-time convergence. The unified design formula of the nonlinear activated ZNN (NAZNN) is presented as

$$\dot{\mathfrak{E}}(t) = -\mu\mathfrak{A}(\mathfrak{E}(t)), \tag{3}$$

where $\mu > 0$, $\mathfrak{A}(\cdot)$ denotes a nonlinear activation function. For the purpose of enabling ZNN to converge in finite time, in 2013, a sign-bi-power activation function (named SBP-AF) was fisrt presented in [25], which actualizes the finite-time convergence. After that, the finite-time convergence of ZNN has been widely investigated [35], [36], [37], [38], [39], [40], [41]. With its further study, the SBP-AF is found that the structure is too redundant, which interferes simulation calculation and hardware implementation. Therefore, for improving the finite-time convergence, the structure of SBP-AF can be further optimized.

Based on the above analysis, it can be concluded that the robustness and finite-time convergence of ZNN can simultaneously investigated by designing a new unified formula combined Eq. (2) and Eq. (3). The purpose of our work is to establish a new nonlinearly activated IEZNN (NIEZNN) model for solving the time-varying Sylvester equation in different noise environments. Three cruces are considered in the design of NIEZNN, one is the stability, to obtain effective computation; the other is the robustness, to own good noise immunity; and the last one is expediting the finite-time convergence, to meet higher requirements in solving time-varying problems. A designed coalescent activation function (C-AF) is embedded to the NIEZNN model, which impels the NIEZNN possess better finite-time convergence and noise suppression in solving the time-varying Sylvester equation. In addition, theoretical conclusions are derived, and the superiority of NIEZNN under additive noise is verified via comparison of numerical experiments and application on controlling mobile manipulator. The novelty and contribution of this paper are summed up as below.

- A general framework of NIEZNN is proposed for solving time-varying Sylvester equation. Besides, a novel nonlinear function is presented to activate the NIEZNN mode, which is more convenient for simulations and calculations.
- The robustness and the finite-time convergence of the NIEZNN model have been proved in theoretical analyses. Furthermore, the upper bounds of convergence time of the NIEZNN model and the noise-attached NIEZNN model have been deduced in theory.
- The existing neural networks are applied to solve time-varying Sylvester equation for comparative purposes, and abundant experimental validations (including the application to mobile manipulators) demonstrate the better finite-time convergence and robustness of the proposed NIEZNN based on a novel C-AF.

II. PROBLEM FORMULATION AND MODEL

In this section, we are concerned with the following time-varying Sylvester equation.

$$A(t)Y(t) - Y(t)B(t) + C(t) = 0, \tag{4}$$

where $A(t)$, $B(t)$ and $C(t)$ present known time-varying matrices, $Y(t)$ is an unknown time-varying matrix.

The aim of our work is to obtain the solution of $Y(t)$ within finite-time in different noises by taking advantage of the NIEZNN. Following the general design procedure of ZNN model, the design process of the NIEZNN model for time-varying Sylvester equation can be obtained as below.

At first, define the error monitoring function:

$$\mathfrak{E}(t) = A(t)Y(t) - Y(t)B(t) + C(t). \tag{5}$$

Then, define a evolution formula for $\mathfrak{E}(t)$, which simultaneously achieves finite-time convergence and noise tolerance. Combining the design characteristics of (2) and (3), a novel evolution formula is defined as following:

$$\dot{\mathfrak{E}}(t) = -\mu\mathfrak{A}_1\big(\mathfrak{E}(t)\big) - \nu\mathfrak{A}_2\Big(\mathfrak{E}(t) + \mu\int_0^t \mathfrak{A}_1(\mathfrak{E}(s))\,\mathrm{d}s\Big), \tag{6}$$

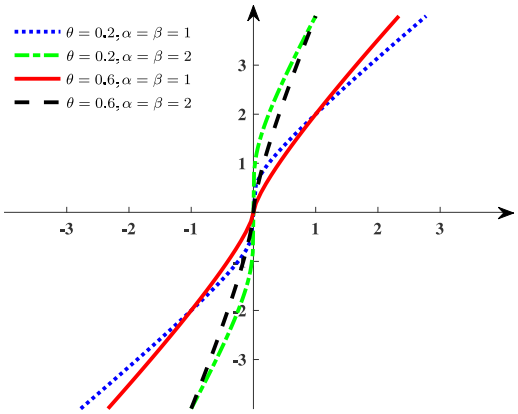

FIGURE 1. The curves of C-AF (7) with different parameters values.

where $\mu > 0$ and $\nu > 0$ are the scale parameters, $\mathfrak{A}_1(\cdot)$ and $\mathfrak{A}_2(\cdot)$ denote the nonlinear activation functions, which are odd and monotone increasing. As we know that the SBP-AF designed in [25] can endow ZNN finite-time convergence, but the structure is too redundant, which interferes simulation calculation and hardware implementation. If we continue to expedite the convergence speed, much efficiency will be sacrificed. Therefore, we propose a new coalescent activation function (named C-AF) combined the simplified form of SBP-AF with a linear activation function as following:

$$\mathfrak{A}(x) = \alpha \mathrm{sgn}^{\theta}(x) + \beta x, \tag{7}$$

where $\mathrm{sgn}^{\theta}(\cdot)$ is defined as

$$\mathrm{sgn}^{\theta}(x) = \begin{cases} |x|^{\theta}, & \text{if } x > 0, \\ 0, & \text{if } x = 0, \\ -|x|^{\theta}, & \text{if } x < 0. \end{cases} \tag{8}$$

To illustrate the proposed C-AF, Fig. 1 plots the curves of the C-AF with different parameters values. From the figure, we can see that the effect of α and β is more significant than θ, a larger value of the parameters α and β prompts function (7) has a faster rate change.

At last, combining (5) and (6), the NIEZNN model is obtained for solving time-varying Sylvester equation.

$$\begin{aligned} A(t)\dot{Y}(t) - \dot{Y}(t)B(t) = {} & Y(t)\dot{B}(t) - \dot{A}(t)Y(t) \\ & - \dot{C}(t) - \mu\mathfrak{A}_1\big(A(t)Y(t) \\ & - Y(t)B(t) + C(t)\big) \\ & - \nu\mathfrak{A}_2\big(A(t)Y(t) - Y(t)B(t) + C(t) \\ & + \mu \int_0^t \mathfrak{A}_1(A(s)Y(s) - Y(s)B(s) \\ & + C(s))\,\mathrm{d}s\big). \end{aligned} \tag{9}$$

As we know that noise is inevitably in the practical environment. In general, especially in noise disturbed situation, a zeroing neural network might develop to an unstable state (e.g. oscillation, divergence and chaos). In this case, noise leads to failure of the computing task. In order to investigate the anti-noise performance of NIEZNN model (9) for solving time-varying Sylvester equation, we extend the NIEZNN model (9) by appending a random noise as follow noise-attached NIEZNN model:

$$\begin{aligned} A(t)\dot{Y}(t) - \dot{Y}(t)B(t) = {} & Y(t)\dot{B}(t) - \dot{A}(t)Y(t) - \dot{C}(t) \\ & - \mu\mathfrak{A}_1\big(A(t)Y(t) - Y(t)B(t) + C(t)\big) \\ & - \nu\mathfrak{A}_2\big(A(t)Y(t) - Y(t)B(t) + C(t) \\ & + \mu \int_0^t \mathfrak{A}_1(A(s)Y(s) - Y(s)B(s) \\ & + C(s))\,\mathrm{d}s\big) + o(t), \end{aligned} \tag{10}$$

where $o(t)$ denotes a random noise matrix, the random noise may be constant noise or time-varying noise.

Remark 1: The parameters μ and ν can adjust the convergence of neural network systems of NIEZNN model (9). A large value of μ and ν can accelerate the convergence. As to the robustness, a large value of μ and ν is apt to make the neural network system sensitive to noise. The integral unit in NIEZNN model (9) can eliminate instability of control systems with additional noise. Therefore, in applications, parameters μ and ν are set as large as hardware permits.

Remark 2: The matrix-form NIEZNN model is transformed into an initial-value ODE problem via MATLAB, which makes simulation and calculation more easy and efficient.

III. ROBUSTNESS AND FINITE-TIME CONVERGENCE ANALYSES

In this section, theoretical analyses are presented, which show the robustness and finite-time convergence of the NIEZNN model with the proposed C-AF (7).

A. ROBUSTNESS

The robustness of NIEZNN model (9) is incarnated by analysing noise-attached NIEZNN model (10).

Theorem 1: In front of an unknown additive noise, the state matrix $Y(t)$ generated by noise-attached NIEZNN model (10) is stable and globally converges to the theoretical solution $Y^*(t)$ of (4), that is to say, $\mathfrak{E}(t)$ will globally converges to zero with time.

Proof: The evolution formula of noise-attached NIEZNN model (10) is presented as

$$\begin{aligned} \dot{\mathfrak{E}}(t) = {} & -\mu\mathfrak{A}_1\big(\mathfrak{E}(t)\big) \\ & - \nu\mathfrak{A}_2\big(\mathfrak{E}(t) + \mu \int_0^t \mathfrak{A}_1(\mathfrak{E}(s))\,\mathrm{d}s\big) + o(t), \end{aligned} \tag{11}$$

the ijth entry of $\dot{\mathfrak{E}}(t)$ of (11) can be obtained as below:

$$\begin{aligned} \dot{\mathfrak{e}}_{ij}(t) = {} & -\mu\mathfrak{A}_1\big(\mathfrak{e}_{ij}(t)\big) \\ & - \nu\mathfrak{A}_2\big(\mathfrak{e}_{ij}(t) + \mu \int_0^t \mathfrak{A}_1(\mathfrak{e}_{ij}(s))\,\mathrm{d}s\big) + o_{ij}(t), \end{aligned} \tag{12}$$

we set

$$\Delta_{ij}(t) = \mathfrak{e}_{ij}(t) + \mu \int_0^t \mathfrak{A}_1(\mathfrak{e}_{ij}(s))\,\mathrm{d}s, \tag{13}$$

the derivative of (13) can be gotten as:

$$\dot{\epsilon}_{ij}(t) = \dot{\Delta}_{ij}(t) - \mu\mathfrak{A}_1(\epsilon_{ij}(t)). \tag{14}$$

Finally, substituting (13),(14) into (12), we have

$$\dot{\Delta}_{ij}(t) = -\nu\mathfrak{A}_2(\Delta_{ij}(t)) + o_{ij}(t), \tag{15}$$

for analyzing the stability of (12), a Lyapunov function candidate is constructed as following

$$S_{ij}(t) = \frac{\left(\nu\mathfrak{A}_2(\Delta_{ij}(t)) - o_{ij}(t)\right)^2}{2}.$$

Obviously, $S_{ij}(t)$ is a positive-definite function, based on $\dot{\epsilon}_{ij}(t) = \dot{\Delta}_{ij}(t) - \mu\mathfrak{A}_1(\epsilon_{ij}(t))$, the derivative of $S_{ij}(t)$ can be computed as

$$\begin{aligned}\dot{S}_{ij}(t) &= (\nu\mathfrak{A}_2(\Delta_{ij}(t)) - o_{ij}(t))\nu\frac{\partial\mathfrak{A}_2(\Delta_{ij}(t))}{\partial\Delta_{ij}}\dot{\Delta}_{ij}(t).\\ &= -\nu\frac{\partial\mathfrak{A}_2(\Delta_{ij}(t))}{\partial\Delta_{ij}}(\nu\mathfrak{A}_2(\Delta_{ij}(t)) - o_{ij}(t))^2.\end{aligned}$$

Because of the given condition that $\mathfrak{A}_2(\cdot)$ is an odd monotone increasing function, we can conclude that $\frac{\partial\mathfrak{A}_2(\Delta_{ij}(t))}{\partial\Delta_{ij}} > 0$, therefore, $\dot{S}_{ij}(t)$ is negative definite. Which means $S_{ij}(t)$ will globally converge to zero with time goes on, i.e.,

$$\lim_{t\to\infty} S_{ij}(t) = \lim_{t\to\infty} \frac{\left(\nu\mathfrak{A}_2(\Delta_{ij}(t)) - o_{ij}(t)\right)^2}{2} = 0,$$

that is equivalent to

$$\lim_{t\to\infty} (\nu\mathfrak{A}_2(\Delta_{ij}(t)) - o_{ij}(t)) = 0.$$

According to Eq.(15), we have the conclusion

$$\lim_{t\to\infty} \dot{\Delta}_{ij}(t) = 0.$$

based on $\dot{\epsilon}_{ij}(t) = \dot{\Delta}_{ij}(t) - \mu\mathfrak{A}_1(\epsilon_{ij}(t))$ again, with the time goes on, we have

$$\dot{\epsilon}_{ij}(t) = -\mu\mathfrak{A}_1\left(\epsilon_{ij}(t)\right),$$

which is the NAZNN design formula, we can construct a Lyapunov function candidate $Z_{ij}(t) = \epsilon_{ij}^2(t)/2$, obviously, $Z_{ij}(t)$ is positive definite. Besides, the derivative of $Z_{ij}(t)$ can be obtained easily as:

$$\dot{Z}_{ij}(t) = \epsilon_{ij}(t)\dot{\epsilon}_{ij}(t) = -\mu\epsilon_{ij}(t)\mathfrak{A}_1\left(\epsilon_{ij}(t)\right),$$

from the given condition that $\mathfrak{A}_1(\cdot)$ is an odd monotone increasing function, we have $\dot{Z}_{ij}(t) \le 0$, i.e., $\dot{Z}_{ij}(t)$ is negative definite, that's to say $\epsilon_{ij}(t)$ globally converge to zero with time going on in noise situation. The proof is completed. □

B. FINITE-TIME CONVERGENCE

Theorem 2: The state matrix $Y(t)$ generated by the NIEZNN model with the proposed C-AF (7) is stable and globally converges to the theoretical solution $Y^*(t)$ of (4) in finite-time

$$t_{up} \le \frac{\mu+\nu}{\mu\nu\beta(1-\theta)}\max\{\ln\frac{\beta \mid \epsilon^+(0)\mid^{1-\theta}+\alpha}{\alpha}, \ln\frac{\beta \mid \epsilon^-(0)\mid^{1-\theta}+\alpha}{\alpha}\},$$

where $\epsilon^+(0)$ and $\epsilon^-(t)$ represent the largest and the smallest values of $\mathfrak{E}(0)$.

Proof: Based on the evolution formula (6), the element of $\dot{\mathfrak{E}}(t)$ can be obtained as below:

$$\dot{\epsilon}(t) = -\mu\mathfrak{A}_1\left(\epsilon(t)\right) - \nu\mathfrak{A}_2\left(\epsilon(t) + \mu\int_0^t \mathfrak{A}_1(\epsilon(s))\,ds\right). \tag{16}$$

Same as the proof of Theorem 1, we also set

$$\Delta(t) = \epsilon(t) + \mu\int_0^t \mathfrak{A}_1(\epsilon(s))\,ds,$$

so we have $\Delta(0) = \epsilon(0)$ when $t = 0$. Besides, we also have

$$\dot{\Delta}(t) = -\nu\mathfrak{A}_2(\Delta(t)),$$

Based on the design of the proposed C-AF (7) and NIEZNN (9) model,

$$\begin{aligned}\dot{\Delta}(t) &= -\nu(\alpha\mathrm{sgn}^\theta(\Delta(t)) + \beta\Delta(t))\\ &= -\nu\alpha\mathrm{sgn}^\theta(\Delta(t)) - \nu\beta\Delta(t),\end{aligned} \tag{17}$$

considering the definition of $\mathrm{sgn}^\theta(\cdot)$ in (8), we have

1) If $\Delta(0) > 0$, (17) can be derived as

$$\dot{\Delta}(t) = -\nu\alpha(\Delta(t))^\theta - \nu\beta\Delta(t),$$

which is equivalent to

$$(\Delta(t))^{-\theta}\frac{\partial\Delta(t)}{\partial t} + \nu\beta(\Delta(t))^{1-\theta} + \nu\alpha = 0. \tag{18}$$

To solve the differential equation (18), we set $\varphi(t) = (\Delta(t))^{1-\theta}$, then

$$\frac{\partial\varphi(t)}{\partial t} = (1-\theta)(\Delta(t))^{-\theta}\frac{\partial\Delta(t)}{\partial t}.$$

So, (18) can be written as

$$\frac{\partial\varphi(t)}{\partial t} + (1-\theta)\nu\beta\varphi(t) + (1-\theta)\nu\alpha = 0.$$

The solution of above differential equation is

$$\varphi(t) = \left(\frac{\alpha}{\beta} + \varphi(0)\right)e^{(1-\theta)\nu\beta t} - \frac{\alpha}{\beta}.$$

As we know that $\Delta(t)$ converges to 0 at the finite time t^*, that is $\Delta(t^*) = 0$ and $\varphi(t^*) = 0$. Thus,

$$\left(\frac{\alpha}{\beta} + \varphi(0)\right)e^{(1-\theta)\nu\beta t^*} - \frac{\alpha}{\beta} = 0.$$

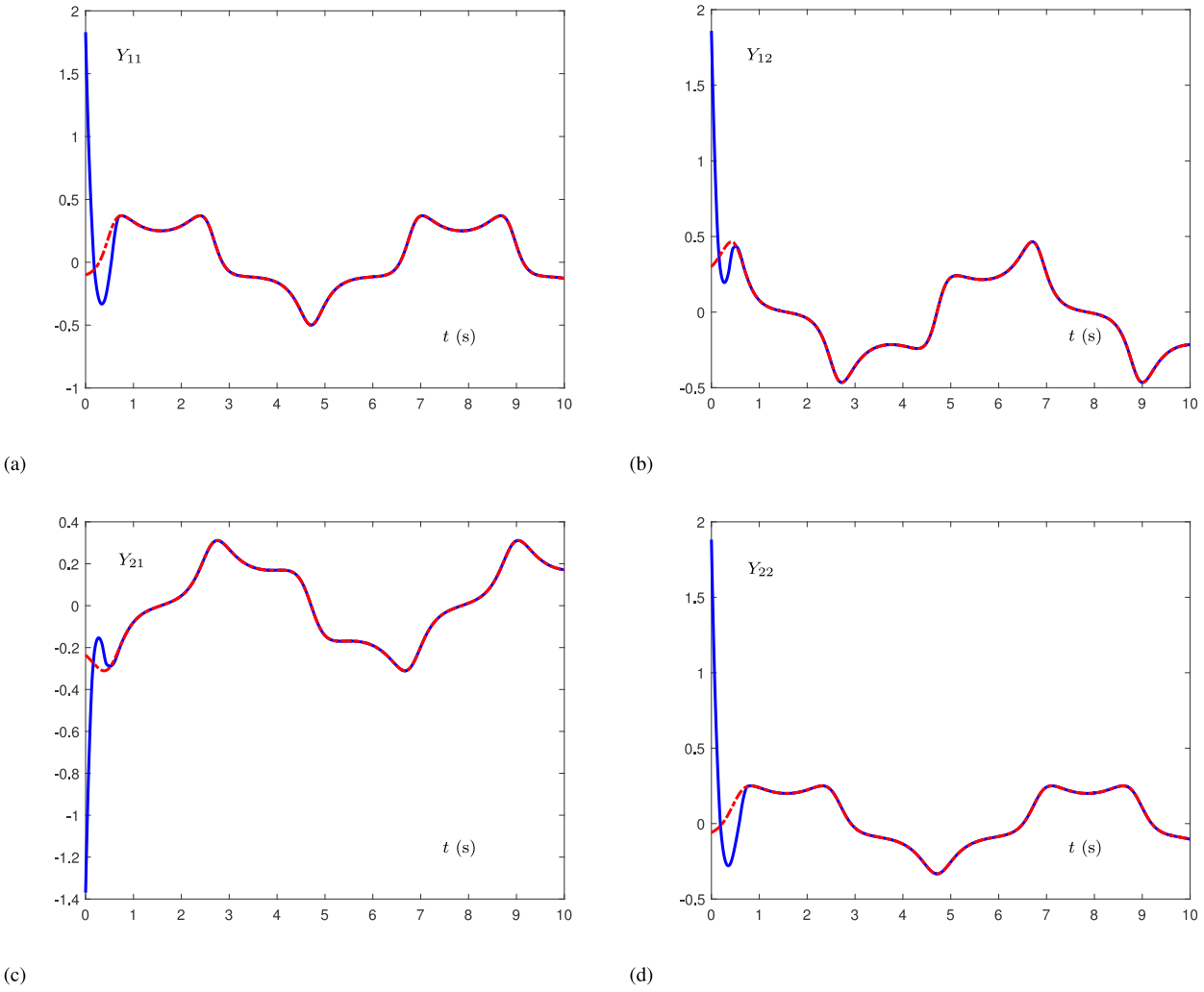

FIGURE 2. Starting from a randomly initial state $Y(0)$, state matrix $Y(t)$ synthesized by the NIEZNN model converges to the theoretical solution precisely and rapidly. The results verify the finite time convergence in Theorem 2.

Solving the above equation, in the case of $\Delta(0) > 0$, we obtain the upper limit of convergence time

$$t^* = \frac{1}{\nu\beta(1-\theta)}\ln\frac{\beta(\Delta(0))^{1-\theta}+\alpha}{\alpha} = \frac{1}{\nu\beta(1-\theta)}\ln\frac{\beta \mid \Delta(0)\mid^{1-\theta}+\alpha}{\alpha}.$$

2) If $\Delta(0) < 0$, similarly, we have the result that

$$t^* = \frac{1}{\nu\beta(1-\theta)}\ln\frac{\beta(-\Delta(0))^{1-\theta}+\alpha}{\alpha} = \frac{1}{\nu\beta(1-\theta)}\ln\frac{\beta \mid \Delta(0)\mid^{1-\theta}+\alpha}{\alpha}.$$

3) If $\Delta(0) = 0$, obviously,

$$t^* = 0 = \frac{1}{\nu\beta(1-\theta)}\ln\frac{\beta \mid \Delta(0)\mid^{1-\theta}+\alpha}{\alpha}.$$

Therefore, we can have the conclusion that $\Delta(t)$ converges to 0 when $t > \frac{1}{\nu\beta(1-\theta)}\max\{\ln\frac{\beta|\Delta^+(0)|^{1-\theta}+\alpha}{\alpha}, \ln\frac{\beta|\Delta^-(0)|^{1-\theta}+\alpha}{\alpha}\}$.

Because of $\Delta(0) = \mathfrak{e}(0)$, for $\Delta(t)$, the upper bound of the finite convergence time t_1 of the NIEZNN model is obtained as

$$t_1 < \frac{1}{\nu\beta(1-\theta)}\max\{\ln\frac{\beta \mid \mathfrak{e}^+(0)\mid^{1-\theta}+\alpha}{\alpha}, \ln\frac{\beta \mid \mathfrak{e}^-(0)\mid^{1-\theta}+\alpha}{\alpha}\}.$$

When $t > t_1$, $\Delta(t) = 0$ and $\dot{\Delta}(t) = 0$, from $\dot{\mathfrak{e}}(t) = \dot{\Delta}(t) - \mu\mathbb{P}_1(\mathfrak{e}(t))$, we have

$$\dot{\mathfrak{e}}(t) = -\mu\mathfrak{A}_1(\mathfrak{e}(t)),$$

adopting the same way in $\dot{\Delta}(t) = -\nu\mathfrak{A}_2(\Delta(t))$, for $\mathfrak{e}(t)$, the upper bound of the finite convergence time t_2 of the NIEZNN model is obtained as

$$t_2 < \frac{1}{\mu\beta(1-\theta)}\max\{\ln\frac{\beta|\mathfrak{e}^+(0)|^{1-\theta}+\alpha}{\alpha}, \ln\frac{\beta|\mathfrak{e}^-(0)|^{1-\theta}+\alpha}{\alpha}\}.$$

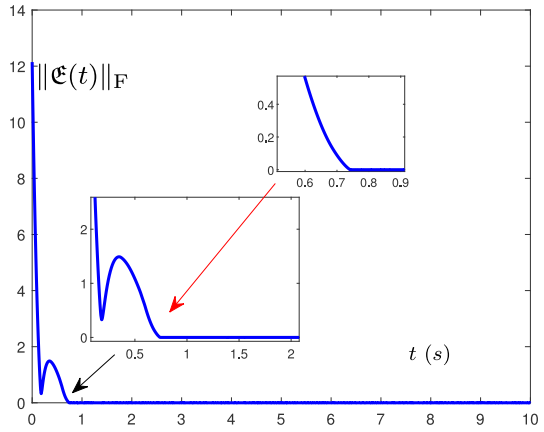

FIGURE 3. Residual errors synthesized by the NIEZNN model embedded C-AF (7).

Finally, we conclude that NIEZNN (9) model can converge to zero in finite time, and the upper bound of convergence time is estimated as

$$\begin{aligned} t_{up} &= t_1 + t_2 \\ &< \frac{\mu+\nu}{\mu\nu\beta(1-\theta)}\max\{\ln\frac{\beta \mid \mathfrak{e}^{+}(0)\mid^{1-\theta}+\alpha}{\alpha}, \\ &\qquad \ln\frac{\beta \mid \mathfrak{e}^{-}(0)\mid^{1-\theta}+\alpha}{\alpha}\}. \end{aligned}$$

The proof completes. □

To investigate the finite-time convergence of noise-attached NIEZNN model (10), we have the following theorem.

Theorem 3. In front of an unknown additive noise $o(t)$ with its element satisfying $o_{ij}(t) \le \varpi$ ($\varpi > 0$), the state matrix $Y(t)$ generated by noise-attached NIEZNN model (10) with the proposed C-AF (7) is stable and globally converges to the theoretical solution $Y^*(t)$ of (4) in finite-time

$$\begin{aligned} t_{up} \le \frac{\mu+\nu}{\mu\nu\beta(1-\theta)}\max\{\ln\frac{\beta \mid \mathfrak{e}^{+}(0)\mid^{1-\theta}+\alpha}{\alpha}, \\ \ln\frac{\beta \mid \mathfrak{e}^{-}(0)\mid^{1-\theta}+\alpha}{\alpha}\}, \end{aligned}$$

where $\mathfrak{e}^{+}(0)$ and $\mathfrak{e}^{-}(t)$ represent the largest and the smallest values of $\mathfrak{E}(0)$.

Proof: Based on the **Theorem 1**, the element of $\dot{\mathfrak{E}}(t)$ can be obtained as below:

$$\dot{\mathfrak{e}}(t) = -\mu\mathfrak{A}_1\big(\mathfrak{e}(t)\big) - \nu\mathfrak{A}_2\Big(\mathfrak{e}(t) + \mu\int_0^t \mathfrak{A}_1(\mathfrak{e}(s))\,\mathrm{d}s\Big) + o(t). \tag{19}$$

We also set $\Delta(t) = \mathfrak{e}(t) + \mu\int_0^t \mathfrak{A}_1(\mathfrak{e}(s))\,\mathrm{d}s$, then, we have

$$\dot{\Delta}(t) = -\nu\mathfrak{A}_2(\Delta(t)) + o(t), \tag{20}$$

where $\mathfrak{A}_2(\cdot)$ adopts the proposed C-AF (7), $o(t)$ is set as $\varpi\,\Delta^{\theta}(t)$. Eq.(20) is represented as:

$$\begin{aligned} \dot{\Delta}(t) &= -\nu(\alpha\mathrm{sgn}^{\theta}(\Delta(t)) + \beta\Delta(t)) + \varpi\,\Delta^{\theta}(t) \\ &= -\nu\alpha\mathrm{sgn}^{\theta}(\Delta(t)) - \nu\beta\Delta(t) + \varpi\,\Delta^{\theta}(t), \end{aligned} \tag{21}$$

according to the definition of $\mathrm{sgn}^{\theta}(\cdot)$ in (8), when $\Delta(0) > 0$, Eq.(21) can be derived as

$$\dot{\Delta}(t) = -\nu\alpha\Delta^{\theta}(t) - \nu\beta\Delta(t) + \varpi\,\Delta^{\theta}(t),$$

which is equivalent to

$$(\Delta(t))^{-\theta}\frac{\partial\Delta(t)}{\partial t} + \nu\beta(\Delta(t))^{1-\theta} + \nu\alpha - \varpi = 0. \tag{22}$$

We set $\varphi(t) = (\Delta(t))^{1-\theta}$, then

$$\frac{\partial\varphi(t)}{\partial t} = (1-\theta)(\Delta(t))^{-\theta}\frac{\partial\Delta(t)}{\partial t},$$

so, Eq.(22) can be written as

$$\frac{\partial\varphi(t)}{\partial t} + (1-\theta)\nu\beta\varphi(t) + (1-\theta)(\nu\alpha - \varpi) = 0. \tag{23}$$

The solution of the differential equation (23) is

$$\varphi(t) = \Big(\frac{\nu\alpha-\varpi}{\nu\beta} + \varphi(0)\Big)e^{(1-\theta)\nu\beta t} - \frac{\nu\alpha-\varpi}{\nu\beta}.$$

As we know that $\Delta(t)$ converges to 0 at the finite time t^*, that is $\Delta(t^*) = 0$ and $\varphi(t^*) = 0$. Thus,

$$\Big(\frac{\nu\alpha-\varpi}{\nu\beta} + \varphi(0)\Big)e^{(1-\theta)\nu\beta t^*} - \frac{\nu\alpha-\varpi}{\nu\beta} = 0.$$

Solving the above equation, in the case of $\Delta(0) > 0$, we obtain the upper limit of convergence time

$$\begin{aligned} t^* &= \frac{1}{\nu\beta(1-\theta)}\ln\frac{\nu\beta(\Delta(0))^{1-\theta}+\nu\alpha-\varpi}{\nu\alpha} \\ &< \frac{1}{\nu\beta(1-\theta)}\ln\frac{\nu\beta(\Delta(0))^{1-\theta}+\nu\alpha}{\nu\alpha} \\ &< \frac{1}{\nu\beta(1-\theta)}\ln\frac{\beta(\Delta(0))^{1-\theta}+\alpha}{\alpha} \\ &= \frac{1}{\nu\beta(1-\theta)}\ln\frac{\beta \mid \Delta(0)\mid^{1-\theta}+\alpha}{\alpha}. \end{aligned}$$

When $\Delta(0) \le 0$, similarly, we have the result that

$$t^* < \frac{1}{\nu\beta(1-\theta)}\ln\frac{\beta \mid \Delta(0)\mid^{1-\theta}+\alpha}{\alpha}.$$

Therefore, we can have the conclusion that $\Delta(t)$ converges to 0 when $t > \frac{1}{\nu\beta(1-\theta)}\max\{\ln\frac{\beta|\Delta^{+}(0)|^{1-\theta}+\alpha}{\alpha}, \ln\frac{\beta|\Delta^{-}(0)|^{1-\theta}+\alpha}{\alpha}\}$. So, the upper bound of the finite convergence time t_1 of the noise-attached NIEZNN model is obtained as

$$\begin{aligned} t_1 < \frac{1}{\nu\beta(1-\theta)}\max\{\ln\frac{\beta \mid \mathfrak{e}^{+}(0)\mid^{1-\theta}+\alpha}{\alpha}, \\ \ln\frac{\beta \mid \mathfrak{e}^{-}(0)\mid^{1-\theta}+\alpha}{\alpha}\}. \end{aligned}$$

When $t > t_1$, $\Delta(t) = 0$ and $\dot{\Delta}(t) = 0$, from $\Delta(t) = \mathfrak{e}(t) + \mu\int_0^t \mathfrak{A}_1(\mathfrak{e}(s))\,\mathrm{d}s$, we have $\dot{\mathfrak{e}}(t) = \dot{\Delta}(t) - \mu\mathbb{P}_1(\mathfrak{e}(t))$, then

$$\dot{\mathfrak{e}}(t) = -\mu\mathfrak{A}_1(\mathfrak{e}(t)),$$

where $\mathfrak{A}_1(\cdot)$ adopts the proposed nonlinear activation function (7), for $\mathfrak{e}(t)$, as **Theorem 2**, the upper bound of the finite

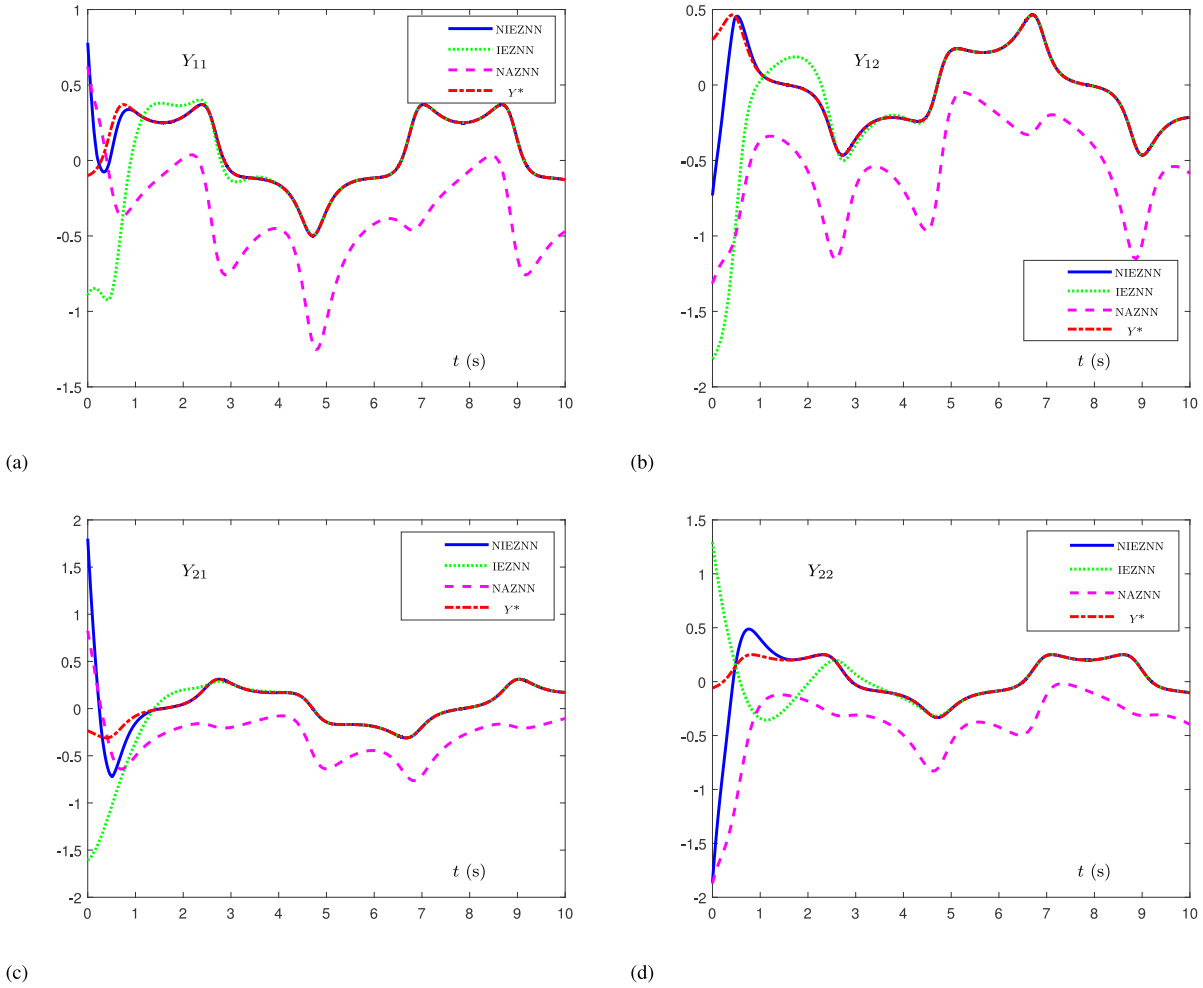

FIGURE 4. State trajectories synthesized by the NIEZNN model, the IEZNN model and the NAZNN model in constant noise $o(t) = 5$, where red dotted curves denote theoretical.

convergence time t_2 of the noise-attached NIEZNN model is obtained as

$$t_2 < \frac{1}{\mu\beta(1-\theta)}\max\{\ln\frac{\beta \mid \mathfrak{e}^+(0)\mid^{1-\theta}+\alpha}{\alpha}, \ln\frac{\beta \mid \mathfrak{e}^-(0)\mid^{1-\theta}+\alpha}{\alpha}\}.$$

Finally, we conclude that noise-attached NIEZNN model (10) can converge to zero in finite time, and the upper bound of convergence time is estimated as

$$\begin{aligned} t_{up} &= t_1 + t_2 \\ &< \frac{\mu+\nu}{\mu\nu\beta(1-\theta)}\max\{\ln\frac{\beta|\mathfrak{e}^+(0)|^{1-\theta}+\alpha}{\alpha}, \ln\frac{\beta|\mathfrak{e}^-(0)|^{1-\theta}+\alpha}{\alpha}\}. \end{aligned}$$

In summary, the finite-time convergence of the noise-attached NIEZNN model is proven. □

IV. SIMULATION AND VERIFICATION

The robustness and finite-time convergence characteristics of NIEZNN model are analyzed in Section III. In this section, numerical experiment results are conducted to validate the superiority of the presented NIEZNN model (9) for solving time-varying Sylvester equation in noise situations. For comparative purposes, on the one hand, the IEZNN, NAZNN and the proposed NIEZNN model are adopted. On the other hand, linear activation function, some representative nonlinear activation functions (including PS-AF and SBP-AF) and the proposed C-AF are embedded in NIEZNN model (9) and noise-attached NIEZNN model (10). Without loss of generality, we set $\theta = 0.2, \alpha = \beta = 1, \mu = \nu = 2$.

Example To solve $Y(t)$ of (4), the coefficients for $A(t)$, $B(t)$ and $C(t)$ are chosen as following

$$A(t) = \begin{bmatrix} \sin(3t) & -\cos(3t) \\ \cos(3t) & \sin(3t) \end{bmatrix},$$
$$B(t) = \begin{bmatrix} 3 & 0 \\ 0 & 4 \end{bmatrix},$$
$$C(t) = \begin{bmatrix} \sin(t) & -\cos(t) \\ \cos(t) & \sin(t) \end{bmatrix}.$$

The effectiveness and accuracy of NIEZNN model (9) are illustrated in Figs.2-3. The overlap of the values synthesized by NIEZNN model (9) and the actual solution is demonstrated in Fig. 2. This figure shows, over a

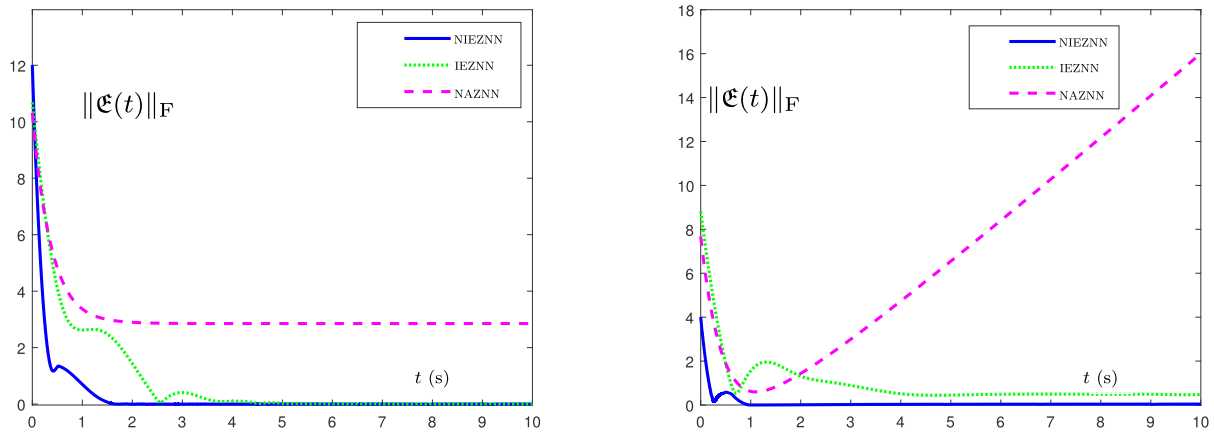

FIGURE 5. Residual errors synthesized by the NIEZNN model, the IEZNN model and the NAZNN model in different noises. (a) In constant noise $o(t) = 5$. (b) In time-varying noise $o(t) = 2t$.

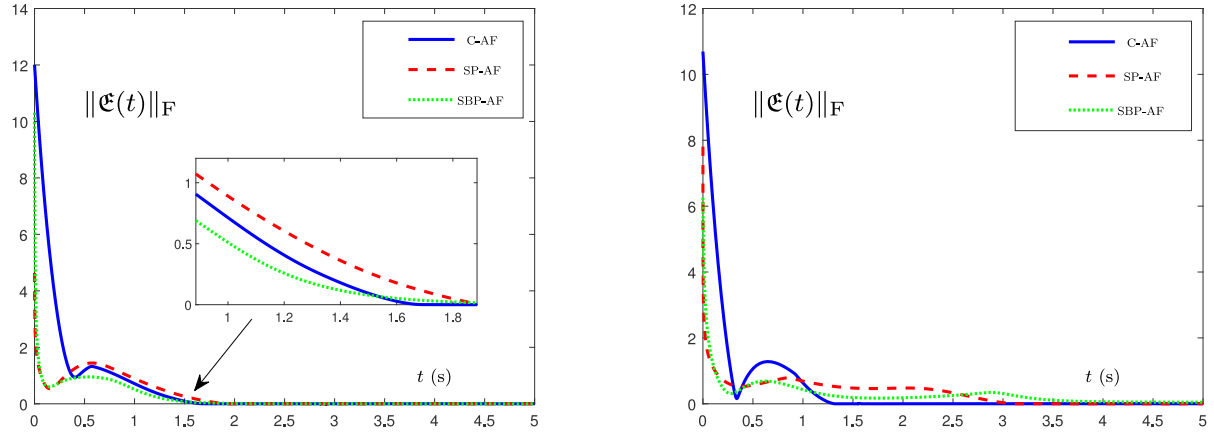

FIGURE 6. Residual errors synthesized by the NIEZNN model with different activation functions in different noises. (a) In constant noise $o(t) = 4$. (b) In time-varying noise $o(t) = t$.

finite-time, the accurate solution of the above time-varying Sylvester equation can be generated by the NIEZNN model. Furthermore, Fig. 3 exhibits the residual error $\|\mathfrak{E}(t)\|_{\mathrm{F}}$ of NIEZNN model (9) can diminish to zero within 0.75 s. which is less than the upper bound $t_{up} \leq \frac{\mu+\nu}{\mu\nu\beta(1-\theta)}\max\{\ln\frac{\beta|\mathfrak{e}^{+}(0)|^{1-\theta}+\alpha}{\alpha}, \ln\frac{\beta|\mathfrak{e}^{-}(0)|^{1-\theta}+\alpha}{\alpha}\} \approx 1.64$ s.

In Figs. 4-5, the superiority of the NIEZNN model on robustness and finite-time is displayed by comparing different models and activation functions. For comparison, the IEZNN model and the NAZNN model are adopted. Fig. 4 illustrates the analytical solutions and the generated solutions by different model with constant noise $o(t) = 5$. The simulation results reveal that the state solution generated by the NAZNN model can not converge the analytical solution in noise situation, the IEZNN model possesses a better robustness but can't achieve finite-time convergence. Although disturbed by noise $o(t) = 5$, the state solution generated by the proposed NIEZNN model rapidly converges to the analytical solution. The corresponding residual error $\|\mathfrak{E}(t)\|_{\mathrm{F}}$ is displayed in Fig. 5(a). For further verification, a linear time-varying noise $o(t) = 2t$ is considered, the simulation results are depicted in Fig. 5(b). When faced time-varying noise, the residual error of the proposed NIEZNN model still quickly converges to zero, which takes no more than 1 s. On the contrary, the residual error of IEZNN model does not decline to zero and remains at approximately 0.8 s. Moreover, the residual error of the NAZNN model keeps climbing over time.

Next, we discuss the choice of activation function. The following two representational activation functions are investigated in NIEZNN model. One is the power-sigmoid activation function (noted PS-AF)

$$\mathfrak{A}(x) = \begin{cases} x^{\lambda} & (\text{with } \lambda \geq 3), \quad \text{if } |x| \geq 1, \\ \frac{1+e^{-\zeta}}{1-e^{-\zeta}} \cdot \frac{1-e^{-\zeta x}}{1+e^{-\zeta x}} & (\text{with } \zeta > 2), \quad \text{if } |x| < 1. \end{cases}$$

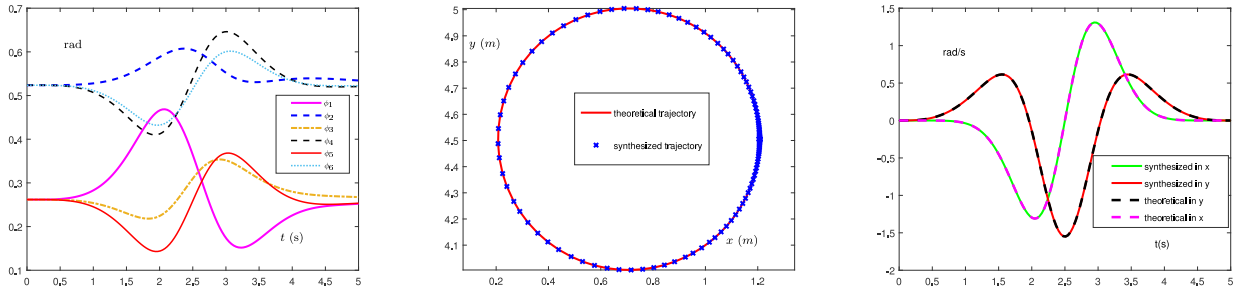

(a) (b) (c)

FIGURE 7. The tracking experiment results synthesized by the control law of the NIEZNN model with $\mu = \nu = 150$ in an additive noise. (a) The path of joint angle. (b) The theoretical and the synthesized trajectory. (c) The comparison between the theoretical and synthesized velocity.

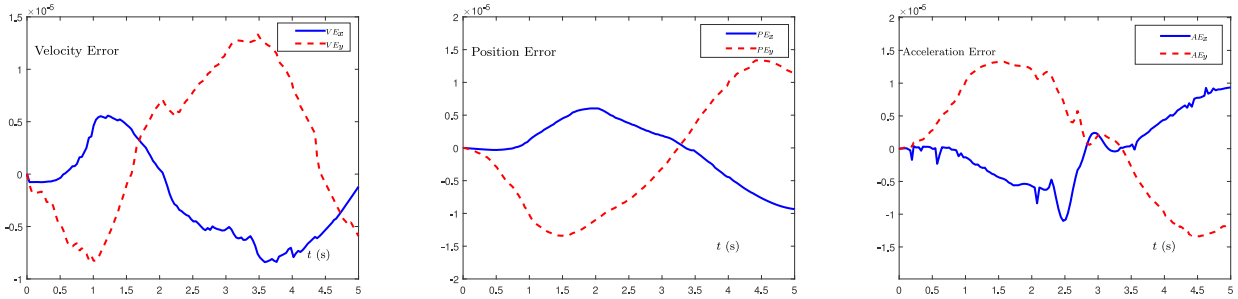

(a) (b) (c)

FIGURE 8. Residual errors synthesized by the control law of the NIEZNN model with $\mu = \nu = 150$ in an additive noise. (a) Velocity error. (b) Position error. (c) Acceleration error.

Another is SBP-AF $\mathfrak{A}(x) = \frac{1}{2}\text{sgn}^{\theta}(x) + \frac{1}{2}\text{sgn}^{1/\theta}(x)$, where the parameter $\theta \in (0, 1)$, and $\text{sgn}^{\theta}(\cdot)$ is defined same as (8). Fig. 6 shows the corresponding experimental results of the NIEZNN model activated by different activation functions for solving time-varying Sylvester equation in noise disturbed situation. In Fig. 6(a), under a constant noise $o(t) = 4$, in Fig. 6(b), under a linear time-varying noise $o(t) = t$. The experimental results verify again the advantages in effectiveness, robustness and finite-time convergence of the proposed NIEZNN model, furthermore, the residual errors of NIEZNN model activated by the designed C-AF converge to zero faster than the same model activated by SP-AF and SBP-AF ($\lambda = 3, \varsigma = 4$) under noise situation. The new C-AF with simpler structure is convenient for simulations and calculations, and what's more, which accelerates convergence speed without remarkable efficiency loss.

V. APPLICATION TO CONTROL MANIPULATOR

In this section, we introduce a mobile manipulator to certify the applicability of the NIEZNN model. The repetitive motion scheme of the mobile manipulator can been found in [42]. The position level, velocity level and the acceleration level can be written as

$$\begin{aligned} \text{minimize} \quad & \frac{1}{2}(\ddot{\phi}(t) + \kappa)^T(\ddot{\phi}(t) + \kappa) \\ \text{subject to} \quad & \mathcal{J}(\phi(t))\ddot{\phi}(t) = \ddot{\omega}_J(t) \end{aligned}$$

where $\kappa := 2\chi\dot{\phi}(t) + \chi^t(\phi(t) - \phi(0))$, here $\chi > 0$, and $\phi(t), \dot{\phi}(t), \ddot{\phi}(t)$ respectively denote the vectors of the manipulator's joint-angle, joint-velocity and joint-acceleration; $\mathcal{J}(\phi(t))$ represents the manipulator's Jacobian matrix; $\ddot{\omega}_J(t) := \ddot{\omega}(t) - \dot{\mathcal{J}}(\phi(t))\dot{\phi}(t)$. Based on the repetitive motion scheme, a kinematics equation can be obtained by using Lagrangian multiplier $\mathfrak{L}(t)$ as

$$M(t)\varrho(t) = \varphi(t),$$

where

$$M(t) := \begin{bmatrix} I & \mathcal{J}^T(t) \\ \mathcal{J}(t) & 0 \end{bmatrix},$$
$$\varrho(t) := \begin{bmatrix} \ddot{\phi}(t) \\ \mathfrak{L}(t) \end{bmatrix}, \varphi(t) := \begin{bmatrix} -\tau \\ \ddot{\omega}_J(t) \end{bmatrix}.$$

Then, we utilize the method of the proposed NIEZNN model to control the motion of the mobile manipulator under the a constant noise $o(t) = 5$. In this simulation experiment, the mobile manipulator is allocated to track a circular route (with the radius being 0.5 m). The initial joint-angle of the mobile manipulator is set as $\phi(0) = [0, 0, \pi/12, \pi/6, \pi/12, \pi/6, \pi/12, \pi/6]^{\text{T}}$, and experimental duration is 5 s. The experiment results synthesized by the NIEZNN model are displayed in Fig. 7-8.

As shown from Fig. 7, the mobile manipulator excellently performs the tracking task. Fig. 7(a) indicates the path

of joint-angle from initial values to final values. Fig. 7(b) indicates the synthesized trajectory overlaps with the theoretical trajectory. Fig. 7(c) depicts simulated velocity the coincides with the theoretical velocity. In addition, Fig. 8 reveals the position error, acceleration error and velocity error are less than 1.4×10^{-5}, the accuracy can meet the needs of practical application. The results of the trajectory-tracking about mobile manipulator fully confirms the design method of the NIEZNN model possesses stronger effectiveness and accuracy.

VI. CONCLUSION

In order to simultaneously promote the robustness and finite-time convergence, a nonlinearly activated integration-enhanced zeroing neural network (NIEZNN) has been designed for solving the time-varying Sylvester equation in various noise situations. In addition, a new coalescent activation function (C-AF) with simpler structure has been designed to embed into the NIEZNN model, which is convenient for hardware implementation, and accelerates convergence speed without remarkable efficiency loss. Furthermore, the robustness and the finite-time convergence of the NIEZNN model have been proved in theoretical analyses. Moreover, the upper bounds of convergence time of the NIEZNN model and the noise-attached NIEZNN model have been deduced in theory. Finally, the advantages of the proposed NIEZNN model based on the designed C-AF have been verified by comparing the NIEZNN model with existing ZNN models for computing time-varying Sylvester equation in noise situations. The comparing results and the application to mobile manipulator have demonstrated the efficiency and superiority of the NIEZNN model and the new coalescent activation function. Compared with fixed parameters, time-varying parameters in ZNN have significant superiority in stability, convergence and robustness. In the future, exploring a delicately time-varying parameter NIEZNN to solve time-varying issues is a valuable direction.

REFERENCES

[1] V. L. Syrmos, "Disturbance decoupling using constrained Sylvester equations," *IEEE Trans. Autom. Control*, vol. 39, no. 4, pp. 797–803, Apr. 1994.

[2] Q. Wei, N. Dobigeon, and J. Tourneret, "Fast fusion of multi-band images based on solving a Sylvester equation," *IEEE Trans. Image Process.*, vol. 24, no. 11, pp. 4109–4121, Nov. 2015.

[3] M. Harker and P. O'Leary, "Least squares surface reconstruction from gradients: Direct algebraic methods with spectral, tikhonov, and constrained regularization," in *Proc. CVPR*, Jun. 2011, pp. 2529–2536.

[4] Z. Zhang, L. Zheng, J. Weng, Y. Mao, W. Lu, and L. Xiao, "A new varying-parameter recurrent neural-network for online solution of time-varying Sylvester equation," *IEEE Trans. Cybern.*, vol. 48, no. 11, pp. 3135–3148, Nov. 2018.

[5] L. Jin, J. Yan, X. Du, X. Xiao, and D. Fu, "RNN for solving time-variant generalized Sylvester equation with applications to robots and acoustic source localization," *IEEE Trans. Ind. Informat.*, vol. 16, no. 10, pp. 6359–6369, Oct. 2020.

[6] E. B. Castelan and V. G. Silva, "On the solution of a Sylvester equation appearing in descriptor systems control theory," *Syst. Control Lett.*, vol. 54, no. 2, pp. 109–117, Feb. 2005.

[7] L. Bao, Y. Lin, and Y. Wei, "A new projection method for solving large Sylvester equations," *Appl. Numer. Math.*, vol. 57, nos. 5–7, pp. 521–532, May 2007.

[8] P. Benner, R.-C. Li, and N. Truhar, "On the ADI method for Sylvester equations," *J. Comput. Appl. Math.*, vol. 233, no. 4, pp. 1035–1045, Dec. 2009.

[9] M. Hajariann, "Matrix iterative methods for solving the Sylvester-transpose and periodic Sylvester matrix equations," *J. Franklin Inst.*, vol. 350, no. 10, pp. 3328–3341, Dec. 2013.

[10] F. Ding and T. Chen, "Iterative least-squares solutions of coupled Sylvester matrix equations," *Syst. Control Lett.*, vol. 54, no. 2, pp. 95–107, Feb. 2015.

[11] Y. Shi, L. Jin, S. Li, J. Li, J. Qiang, and D. K. Gerontitis, "Novel discrete-time recurrent neural networks handling discrete-form time-variant multi-augmented Sylvester matrix problems and manipulator application," *IEEE Trans. Neural Netw. Learn. Syst.*, vol. 33, no. 2, pp. 587–599, Feb. 2022.

[12] R. H. Bartels and G. W. Stewart, "Solution of the matrix equation AX + XB = C [F4]," *Commun. ACM*, vol. 15, no. 9, pp. 820–826, Sep. 1972.

[13] G. Golub, S. Nash, and C. Van Loan, "A hessenberg-schur method for the problem AX + XB= C," *IEEE Trans. Autom. Control*, vol. AC-24, no. 6, pp. 909–913, Dec. 1979.

[14] M. Monsalve, "Block linear method for large scale Sylvester equations," *Clinics*, vol. 27, no. 1, pp. 47–59, 2008.

[15] Z. L. Tian, M. Tian, C. Gu, and X. Hao, "An accelerated Jacobi-gradient based iterative algorithm for solving Sylvester matrix equations," *Filomat*, vol. 31, no. 8, pp. 2381–2390, Jan. 2017.

[16] H. Zhang and H. Yin, "Conjugate gradient least squares algorithm for solving the generalized coupled Sylvester matrix equations," *Comput. Math. with Appl.*, vol. 73, no. 12, pp. 2529–2547, Jun. 2017.

[17] W. Zhang and D. Zhou, "Coupled iterative algorithms based on optimisation for solving Sylvester matrix equations," *IET Control Theory Appl.*, vol. 13, no. 4, pp. 584–593, Mar. 2019.

[18] G. Wang, H. Huang, J. Yan, Y. Cheng, and D. Fu, "An integration-implemented Newton-raphson iterated algorithm with noise suppression for finding the solution of dynamic Sylvester equation," *IEEE Access*, vol. 8, pp. 34492–34499, 2020.

[19] K. Wang, T. Sun, and Y. Dou, "An adaptive learning rate schedule for SIGNSGD optimizer in neural networks," *Neural Process. Lett.*, vol. 54, no. 2, pp. 803–816, Apr. 2022.

[20] D. Chen, Y. Zhang, and S. Li, "Zeroing neural-dynamics approach and its robust and rapid solution for parallel robot manipulators against superposition of multiple disturbances," *Neurocomputing*, vol. 275, pp. 845–858, Jan. 2018.

[21] M. Liu, X. Zhang, M. Shang, and L. Jin, "Gradient-based differential *kWTA* network with application to competitive coordination of multiple robots," *IEEE/CAA J. Automat. Sinica*, vol. 9, no. 8, pp. 1452–1463, Aug. 2022.

[22] S. Li, B. Liu, and Y. Li, "Selective positive–negative feedback produces the winner-take-all competition in recurrent neural networks," *IEEE Trans. Neural Netw. Learn. Syst.*, vol. 24, no. 2, pp. 301–309, Feb. 2012.

[23] C.-A. Popa, "Learning algorithms for quaternion-valued neural networks," *Neural Process. Lett.*, vol. 47, no. 3, pp. 949–973, Jun. 2018.

[24] Y. Zhang, D. Jiang, and J. Wang, "A recurrent neural network for solving Sylvester equation with time-varying coefficients," *IEEE Trans. Neural Netw.*, vol. 13, no. 5, pp. 1053–1063, Sep. 2002.

[25] S. Li, S. Chen, and B. Liu, "Accelerating a recurrent neural network to finite-time convergence for solving time-varying Sylvester equation by using a sign-bi-power activation function," *Neural Process. Lett.*, vol. 37, no. 2, p. 189–205, Apr. 2013.

[26] K. Li, C. Jiang, X. Xiao, H. Huang, Y. Li, and J. Yan, "Residual error feedback zeroing neural network for solving time-varying Sylvester equation," *IEEE Access*, vol. 10, pp. 2860–2868, 2022.

[27] L. Jin, Y. Zhang, and S. Li, "Integration-enhanced Zhang neural network for real-time-varying matrix inversion in the presence of various kinds of noises," *IEEE Trans. Neural Netw. Learn. Syst.*, vol. 27, no. 12, pp. 2615–2627, Dec. 2015.

[28] D. Guo, Z. Nie, and L. Yan, "The application of noise-tolerant ZD design formula to robots' kinematic control via time-varying nonlinear equations solving," *IEEE Trans. Syst., Man, Cybern. Syst.*, vol. 48, no. 12, pp. 2188–2197, Dec. 2017.

[29] Y. Zhang, W. Ma, and B. Cai, "From Zhang neural network to Newton iteration for matrix inversion," *IEEE Trans. Circuits Syst. I, Reg. Papers*, vol. 56, no. 7, pp. 1405–1415, Jul. 2008.

[30] L. Xiao and Y. Zhang, "Zhang neural network versus gradient neural network for solving time-varying linear inequalities," *IEEE Trans. Neural Netw.*, vol. 22, no. 10, pp. 1676–1684, Oct. 2011.

[31] C. Yi, Y. Chen, and Z. Lu, "Improved gradient-based neural networks for online solution of Lyapunov matrix equation," *Inf. Process. Lett.*, vol. 111, no. 16, pp. 780–786, Aug. 2011.
[32] D. Guo, F. Xu, and L. Yan, "New pseudoinverse-based path-planning scheme with PID characteristic for redundant robot manipulators in the presence of noise," *IEEE Trans. Control Syst. Technol.*, vol. 26, no. 6, pp. 2008–2019, Nov. 2017.
[33] L. Xiao and B. Liao, "A convergence-accelerated Zhang neural network and its solution application to Lyapunov equation," *Neurocomputing*, vol. 193, pp. 213–218, Jun. 2016.
[34] J. Jin, J. Zhu, J. Gong, and W. Chen, "Novel activation functions-based ZNN models for fixed-time solving dynamirc Sylvester equation," *Neural Comput. Applic.*, vol. 34, pp. 1–19, Jan. 2022.
[35] B. Liao, Y. Wang, W. Li, C. Peng, and Q. Xiang, "Prescribed-time convergent and noise-tolerant Z-type neural dynamics for calculating time-dependent quadratic programming," *Neural Comput. Appl.*, vol. 33, no. 10, pp. 5327–5337, May 2021.
[36] W. Li, Z. Su, and Z. Tan, "A variable-gain finite-time convergent recurrent neural network for time-variant quadratic programming with unknown noises endured," *IEEE Trans. Ind. Informat.*, vol. 15, no. 9, pp. 5330–5340, Sep. 2019.
[37] D. Guo, F. Xu, Z. Li, Z. Nie, and H. Shao, "Design, verification, and application of new discrete-time recurrent neural network for dynamic nonlinear equations solving," *IEEE Trans. Ind. Informat.*, vol. 14, no. 9, pp. 3936–3945, Sep. 2017.
[38] Y. Shen, P. Miao, Y. Huang, and Y. Shen, "Finite-time stability and its application for solving time-varying Sylvester equation by recurrent neural network," *Neural Process. Lett.*, vol. 42, no. 3, pp. 763–784, 2015.
[39] Z. Jian, L. Xiao, J. Dai, Z. Tang, and C. Liu, "Design and analysis of new zeroing neural network models with improved finite-time convergence for time-varying reciprocal of complex matrix," *IEEE Trans. Ind. Informat.*, vol. 16, no. 6, pp. 3838–3848, Jun. 2019.
[40] L. Xiao, B. Liao, S. Li, and K. Chen, "Nonlinear recurrent neural networks for finite-time solution of general time-varying linear matrix equations," *Neural Netw.*, vol. 98, pp. 102–113, Feb. 2018.
[41] L. Xiao, J. Tao, J. Dai, Y. Wang, L. Jia, and Y. He, "A parameter-changing and complex-valued zeroing neural-network for finding solution of time-varying complex linear matrix equations in finite time," *IEEE Trans. Ind. Informat.*, vol. 17, no. 10, pp. 6634–6643, Oct. 2021.
[42] Z. Zhang, T. Fu, Z. Yan, L. Jin, L. Xiao, Y. Sun, Z. Yu, and Y. Li, "A varying-parameter convergent-differential neural network for solving joint-angular-drift problems of redundant robot manipulators," *IEEE ASME Trans. Mechatronics*, vol. 23, no. 2, pp. 679–689, Jan. 2018.

YIHUI LEI received the Ph.D. degree in statistics from Central South University, Changsha, China, in 2019.

She is currently an Associate Professor with the College of Mathematics and Statistics, Jishou University. Her research interests include neural networks, machine learning, and economic statistics.

JIAMEI LUO is currently pursuing the graduate degree with the College of Mathematics and Statistics, Jishou University. Her main research interest includes neural networks.

TENGXIAO CHEN is currently pursuing the graduate degree with the College of Mathematics and Statistics, Jishou University. His main research interest includes neural networks.

LEI DING received the Ph.D. degree in control science and engineering from Central South University, Changsha, China, in 2009.

He is currently a Professor with the College of Computer Science and Engineering, Jishou University. He has published over 20 articles in various journals/conferences. His current research interests include network security and artificial intelligence.

BOLIN LIAO received the Ph.D. degree in communication and information systems from Sun Yat-sen University, Guangzhou, China, in 2015.

He is currently a Professor with the College of Computer Science and Engineering, Jishou University. He has published around 70 papers in various journals/conferences. His current research interests include neural networks, robotics, and nonlinear control.

GUANGPING XIA is currently pursuing the graduate degree with the College of Mathematics and Statistics, Jishou University. Her main research interest includes neural networks.

ZHENGQI DAI is currently pursuing the graduate degree with the College of Mathematics and Statistics, Jishou University. Her main research interest includes neural networks.